RESEARCH ARTICLE

Design and Development of Solid Lipid Nanoparticles of Tofacitinib Citrate for the Treatment of Rheumatoid Arthritis: A Quality by Design Approach

V Deepika[1*], S Srinu Naik[2]

[1]*Department of Pharmacy, University College of Technology, Osmania University, Hyderabad, Telangana, India.*
[2]*Department of Chemical Engineering, University College of Technology, Osmania University, Hyderabad, Telangana, India.*

Received: 24th February, 2024; Revised: 18th April, 2024; Accepted: 10th June, 2024; Available Online: 25th September, 2024

ABSTRACT

Solid lipid nanoparticles, or SLNs, have gained popularity recently as a possible drug delivery method. However, the idea of using SLNs for organ and site-specific drug administration is still in its early stages due to the difficulties associated with this approach. The aim of this study is to develop SLNs with improved pharmaceutical characterization and anti-arthritic efficacy. Tofacitinib citrate (TC)-loaded SLNs were created using the microemulsification method, with the addition of stearic acid, chitosan, and Tween 80 to improve skin permeability. Seventeen SLNs were developed and characterized for particle size, entrapment efficiency (EE), and percentage drug release according to the Box-Behnken design. The DSC analysis revealed a strong endothermic peak at 166.18°C, significantly different from the pure TC reported at 218.05°C. This indicates a notable alteration in the endothermic peak of the SLNs, demonstrating a relationship with the excipients used in this investigation. XRD study highlighted significant characteristic drug peaks at positions 21.06 and 23.63 (2ɵ). These peaks represented the modifications that were seen in pure TC. The SEM analysis of the optimized lipid nanoparticles showed a smooth surface and a spherical appearance. The particle size analysis of the optimized formulation showed an average size of 181.5 nm. Also, the polydispersity index (PI) revealed a value of 0.495, indicating homogeneous dispersion. The zeta value was 8.2 mV, indicating stability.

Keywords: Tofacitinib citrate, Micro emulsification, Solid lipid nanoparticles, Box-Behnken design, Stability

International Journal of Drug Delivery Technology (2024); DOI: 10.25258/ijddt.14.3.31

How to cite this article: Deepika V, Naik SS. Design and Development of Solid Lipid Nanoparticles of Tofacitinib Citrate for the Treatment of Rheumatoid Arthritis: A Quality by Design Approach. International Journal of Drug Delivery Technology. 2024;14(3):1479-1486.

Source of support: Nil.

Conflict of interest: None

INTRODUCTION

A chronic, systemic inflammatory illness that is pathologically complex, rheumatoid arthritis (RA) can cause irreversible joint deformity and destruction.[1-3] In 2012, the first Janus kinase (JAK) inhibitor, tofacitinib, was approved by the US Food and Drug Administration (USFDA) to treat RA.[4] Crucially, tofacitinib can also regulate synovitis, structural joint degeneration, and T-cell activation.[5] Oral tofacitinib dosage of 5 mg is administered twice a day.[6,7] Tofacitinib lowers the immune system and increases susceptibility to infections when taken orally at large doses (5 mg and 10 mg daily). To effectively distribute tofacitinib, it is necessary to investigate alternative methods of administration. Clinical trials have recently demonstrated good therapeutic effects for the treatment of psoriasis symptoms when 2% tofacitinib ointment is applied topically.[8,9] Tofacitinib applied topically can circumvent the drawbacks of oral therapy. Tofacitinib is also required at a lower dose for topical and transdermal administration than for oral administration,[10] which lessens the likelihood of systemic side effects.[11-13]

For topical and transdermal distribution, the stratum corneum serves as a barrier.[14] Merely a barrier preventing drugs from passing through the skin is formed by corneocytes in the intercellular matrix that makes up the skin. Lipid-based nanocarriers, such as SLNs, have been established to augment drug penetration through the skin.[15-17] Moreover, the factor interaction and its effects on dependent attributes (Table1) were investigated using the design of the experiment (DoE).[18-20] The suggested technology is easy to use and reasonably priced for quantifying tofacitinib in nanoformulations, making it ideal for both industry and academia. It assesses the stability, *in-vitro* release profile, and entrapment efficiency of SLNs loaded with tofacitinib.[21-24]

**Author for Correspondence: deepikavinugala@gmail.com*

Table 1: Factors considered and their quantities

Factor	*Term*	*Coded Low.*	*Coded High.*
A	Stearic acid (%)	-1 ↔ 0.50	+1 ↔ 2.00
B	Chitosan (g)	-1 ↔ 5.00	+1 ↔ 10.00
C	Tween-80 (%)	-1 ↔ 0.10	+1 ↔ 0.50

MATERIALS AND METHODS

Materials

Unison Pharmaceuticals, Baddi, India, provided a free sample of tofacitinib citrate. We purchased stearic acid, chitosan, Tween 80, and glycerol from Fizmerk Chemicals in Uttar Pradesh, India.

Methods

Solid lipid nanoparticle preparation by microemulsification

The Solid lipid nanoparticles are prepared based on a suggestion by BBD. Initially, Stearic acid was melted in a porcelain dish, and Tween 80 was added and gently mixed to obtain the lipid phase.[25,26] Tofacitinib citrate was dissolved in dimethyl sulfoxide (DMSO) in another beaker. The drug solution was then poured into the lipid phase and agitated thoroughly. Meanwhile, various percentages of aqueous solution of chitosan (chitosan in 2% acetic acid solution) were prepared, and the temperature was maintained at 70°C. The lipid phase was added gently with continuous stirring in a mechanical stirrer (Remi stirrer, Mumbai, India) to obtain a hot o/w microemulsion.[27-29] Finally, the hot microemulsion was dispersed into cold water (2–5°C) with continuous stirring at a suitable RPM as per BBD for 1-hour to obtain solid lipid nanoparticles (SLN). The dispersion was further sonicated in a probe sonicator (UAI-PS20khz-900W, Ultra Autosonic, India) for 15 minutes at 20% amplitude to stabilize the lipid nanoparticle dispersion. To get the final volume of 100 mL, the required volume of distilled water was used.

Formulations proposed by the box-behnken design (BBD)

A V-level, three-factor Box-Behnken experimental design of 17 experimental runs was employed in this work. Three separate variables, including Tween-80 (C), chitosan (B), and sodium stearate (A), were taken into consideration.[30-33] Particle size, EE, drug release in the eighth hour, and other responses were noted during the trial shown in Table 2. The polynomial equation was used to fit and analyze mathematical models. Alpha 0.05 was used as the confidence interval value for the numerical approach and graphical optimization methodology to solve the optimized formula.[34]

Characterization of nanoparticles

A precisely weighed quantity of nanoparticles (equal to 10 mg of drug) was added to a 100 mL volumetric flask, and some ethanol was added in small amounts and thoroughly blended. About ten minutes were spent sonicating the dispersion (Ultrasonicator, CPX3800-E, Branson). Phosphate buffer (pH 6.8) was added to the finished formulation, and the volume was adjusted to the necessary amount.[35] After an additional ten minutes of bath sonication, the dispersion turned transparent. A After that, a Whatman membrane filter with a pore size of 0.45 m was used to filter the mixture. The filtrate was subjected to analysis at 289 nm by a UV-vis spectrophotometer (Shimadzu UV-1800, Japan) to determine the quantity of drug present.

Drug loading

$$DL\ (\%) = \frac{\text{Drug content in nanoparticle}}{\text{Total weight of nanoparticle}} \times 100 \quad \text{.....(Equation 1)}$$

Entrapment efficiency

$$EE\ (\%) = \frac{\text{Mass of drug in nanoparticle}}{\text{Initial mass of drug used in nanoparticle}} \times 100 \quad \text{.....(Equation 2)}$$

In-vitro drug release

Franz-diffusion cell was employed to conduct the *in-vitro* drug release of TC from the nanoparticles utilizing the diffusion technique. Before usage, both the dialysis and cellophane membranes were cut into equal sections (6 cm x 2.5 cm) and saturated in distilled water for 12 hours.[36] The TC solution is subjected to drug release experiments in 10 milliliters of phosphate buffer pH 6.8 saline, which is continuously heated using an IKA Auto Temp Regulator (Germany) and magnetic stirrer at 37 ± 0.5°C. The receptor section was filled with a sample of 2 milliliters of nanoparticle suspension. At regular intervals, a milliliter aliquot sample was removed and replaced with the equivalent volume of fresh buffer.[37] The aliquots were diluted, if necessary, by adding fresh medium. Employing a UV spectrophotometer at 289 nm, the amount of drug that permeated the membrane was determined.

Attenuated Total Reflection (ATR) Study

For monitoring of polymer composition, ATR spectroscopy is especially helpful.[38,39] The components of a chemical process can be identified using infrared radiation (IR) because of its capacity to fingerprint chemical compounds. Bruker Opus 7.0, Germany's ATR conducted the investigation.

Differential Scanning Calorimetry (DSC) Study

Temperature and sample physical parameters are measured against time using a DSC (Shimadzu USA's DSC-60), a thermal analysis device.[40,41] As mentioned, this device records temperature and heat flux associated with material changes concerning time and temperature. This is a thermal analysis device.

This is an X-ray diffraction (XRD) Study

By examining the crystal structure of a material, XRD analysis (ARL EQUINOX 100, Thermo Scientific, India) can determine which crystalline phases are present and uncover details about the material's chemical makeup.[42-44]

Surface morphology, Particle size, and zeta potential

Using a scanning electron microscope, the morphology of the transdermal patch loaded with optimized Tofacitinib citrate nanoparticles was examined. Photomicrographs were acquired using a scanning electron microscope (S3700N-Hitachi, Japan) at various magnifications after the sample was adhered to the slab surface using double-sided adhesive tape. A similar

Table 2: Formulation table by box-behnken design

Run	Factor 1	Factor 2	Factor 3	Response 1	Response 2	Response 3
	A:Stearic acid	B:Chitosan	C:Tween-80	EE	Particle size	Percentage drug release at 8h
	%	gm	%	%	nm	%
1	1.25	7.5	0.3	60.47	170	79.57
2	0.5	7.5	0.5	54.17	182	92.38
3	0.5	7.5	0.1	55.32	161	89.12
4	2	7.5	0.5	62.08	193	68.55
5	1.25	7.5	0.3	59.37	171	80.01
6	2	5	0.3	50.89	197	71.35
7	1.25	5	0.1	47.17	194	84.28
8	0.5	5	0.3	40.37	165	99.84
9	1.25	10	0.5	63.68	189	76.27
10	0.5	10	0.3	66.74	173	87.35
11	1.25	7.5	0.3	59.71	175	79.93
12	1.25	7.5	0.3	59.92	169	80.13
13	2	7.5	0.1	64.59	187	66.74
14	1.25	7.5	0.3	60.65	171	80.18
15	1.25	10	0.1	70.27	185	73.58
16	2	10	0.3	74.37	209	64.73
17	1.25	5	0.5	46.53	188	85.67

technique of measuring light scattering intensity was used to assess the particle size and polydispersity index value of nanoparticles using the Malvern Zeta Sizer (ATA Scientific, USA).

RESULTS AND DISCUSSION

In-vitro Drug Release

Formulations as per BBD underwent dissolution for a maximum time of 8h. All formulations released a minimum of 10% in the initial 30 minutes except F13 and F16. F16 released at least 5.98% of drugs at 30 minutes and 64.73% at the 8th hour. However, F8 exhibited a maximum of 99.84% of drugs in the 8th hour. A comparison was made between F2 and F5; both formulations have the same composition but F5 contained a higher 1.25% of stearic acid. It found that F2 released 92.38% of the drug, but F5 released only 80.01% of the drug. This indicated a high amount of stearic acid hindered drug release as it is hydrophobic. Similarly, it also observed for the percentage effect of chitosan in drug dissolution studies. A careful comparison was made between F7 and F15; F7 exhibited 84.28% of the drug at the 8th hour, whereas F15 released only 73.58%. The delay in release from F15 could be attributed to the comparatively high amount of chitosan (10 mg), which formed a layer surrounding the dosage form and delayed drug release. It was also observed a significant contribution of Tween 80 in the percentage of drug release. It found a higher amount of Tween 80 facilitated faster as can be found in F2 and F3. F2 exhibited higher drug release with 0.5%. However, F3 showed only 89.12% of the drug release with 0.1% of Tween 80. Drug loading % shown in Table 3.

Table 3: Drug loading of formulations F1-F17

Run	Drug loading (%)	Run	Drug loading (%)
F1	65.86	F10	71.74
F2	59.46	F11	64.46
F3	60.97	F12	65.27
F4	67.24	F13	69.39
F5	64.17	F14	65.16
F6	55.73	F15	75.55
F7	52.19	F16	79.71
F8	45.64	F17	51.92
F9	68.81		

Model Validation

Response 1 [EE]=60.024+4.416A+11.262B-1.361C-0.72AB-0.34AC -1.48BC+0.098A^2-2.029B^2-1.082C^2 ……..(1)

In Response 1: Term A, Term B, Term C, and B^2 are important.

Response 2 [Particle size] = 171.2+13.125A+1.5B+3.125C+1.0AB-3.75AC +2.5BC+3.275A^2+11.525B^2+6.275C^2…….. (2)

In Response 2: Term A and Quadratic term B^2 are significant as shown in Figure 1.

Response 3 [% Drug release at 8h]= 79.964-12.165A-4.901B+1.143C+1.465AB-0.362AC +0.325BC+0.05A^2+0.803B^2-0.817C^2……..(3)

In Response 3: Term A, Term B, Term C, Interaction term AB, and Quadratic term C^2 are significant, as shown in Figure 2.

Figure 3. depicts the 3d simulation curve & 2D contour plot of response 3 (%drug release at 8h) by using different polymers.

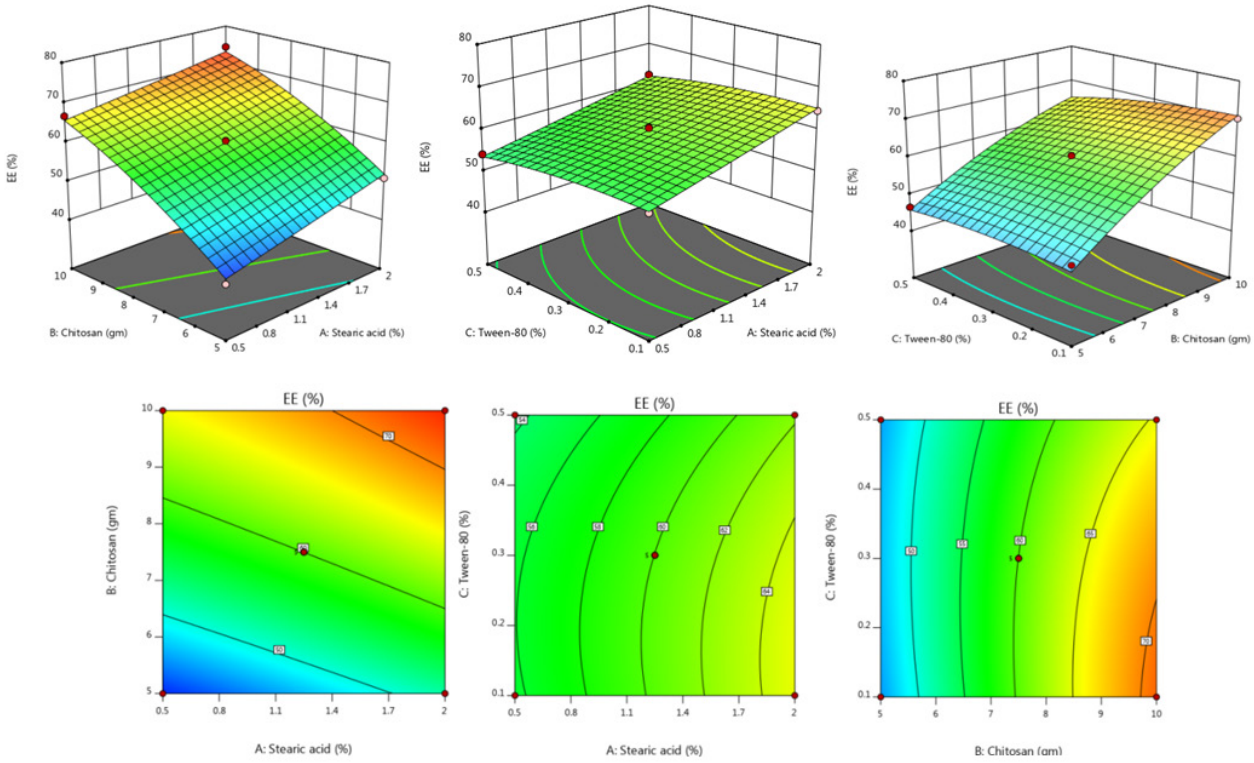

Figure 1: 3D simulation curve of and 2D Contour plot of Response 1(EE)

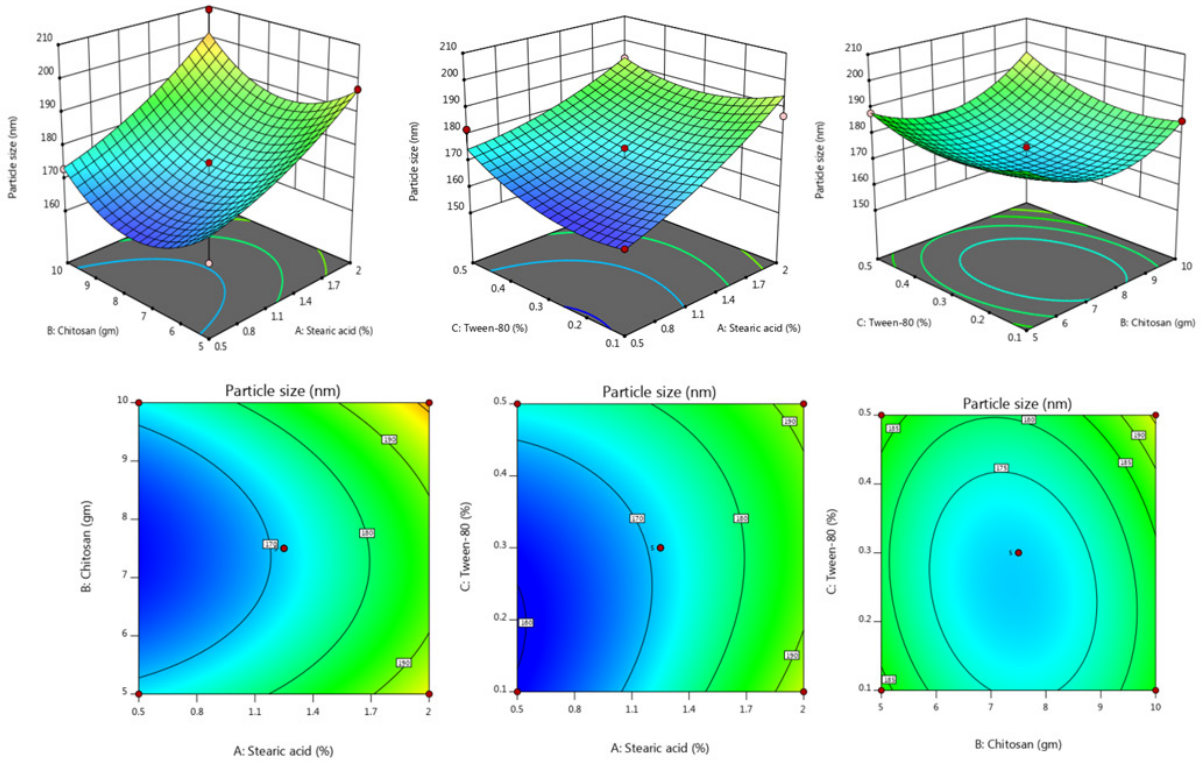

Figure 2: 3D simulation curve & 2D Contour plot of Response 2(Particle size)

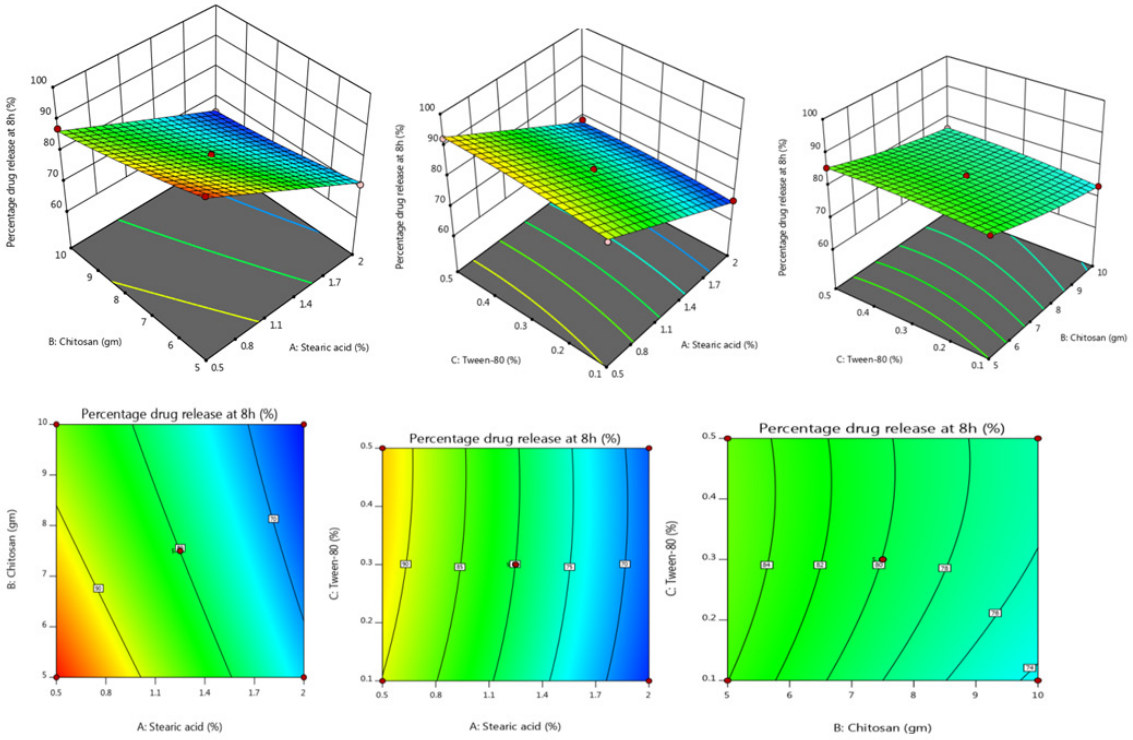

Figure 3: 3D simulation curve & 2D Contour plot of Response 3 (%drug release at 8h)

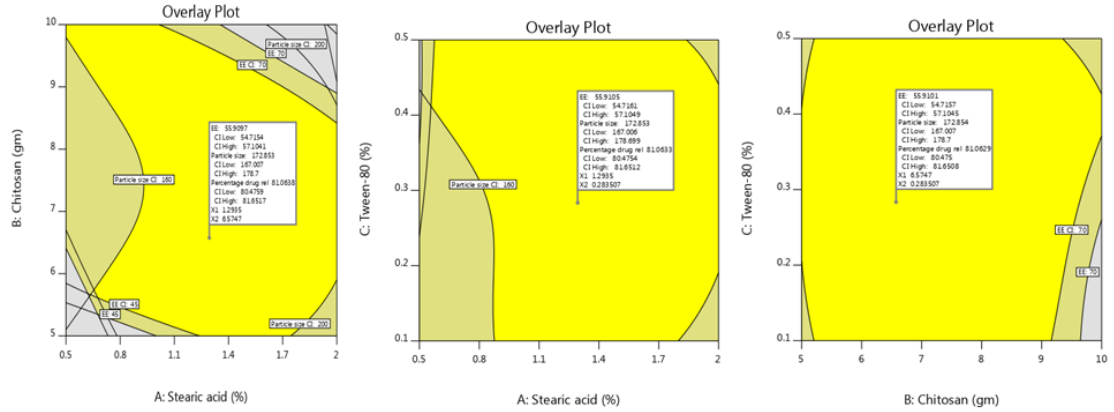

Figure 4: An overlay graphic of the region that shows the values and optimal space

Optimization of Study (Shown in Table 4)

The optimized SLN was prepared and responses were recorded as observed values as shown in Figure 4. The observed value and predicted mean (obtained from response surface simulation) were compared.

Table 4: Optimised formulation's point prediction table

Response	*Observed*	*Std dev*
EE	62.07	1.43221
Particle size	181.5	7.01071
Percentage drug release at 8h	84.28	0.704982

ATR Study

TC comprises three major structural units, which are pyrrole, pyrimidine, and piperidine. The IR peaks were identified and correctly interpreted. A maximum of 1731.26 cm^{-1} due to C=C stretching and a maximum of 841.45 cm^{-1} owing to C-H stretching. Due to C-N stretching in the pyrrole ring, a strong peak emerged at 1207.00 cm^{-1}. Similarly, a peak contributed by N-H stretching in pyrrole emerged at 3497.76 cm^{-1}. At 3367.48 cm^{-1}, a peak emerged in the piperidine ring, which was attributed to N-H stretching, as shown in Figure 5. The carbonyl (C=O) group is responsible for the peak at 1619.80 cm^{-1}. In addition, a prominent distinctive peak at 1341.02 cm^{-1} was noticed, caused by C-N stretching in the pyrimidine ring.

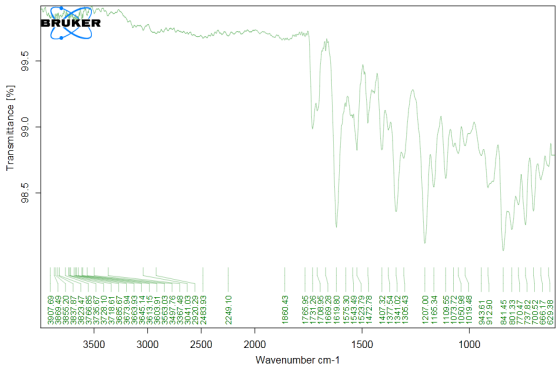

Figure 5: ATR spectra of Tofacitinib citrate

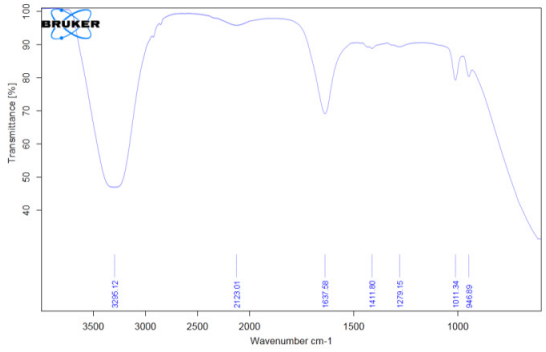

Figure 6: ATR spectra of optimized formulation

The optimized formulation characteristic peaks appeared at 3295.12, 2123.01, 1637.58 and 1011.34 $cm^{-1,}$ as shown in Figure 6.

DSC Study

Figure 7 depicts that a strong endothermic peak was seen in the DSC analysis at 166.18°C, which is significantly different from the pure TC as previously reported at 218.05°C. A noteworthy alteration in the endothermic peak was determined, and this suggested a relationship with the excipients taken into account in this investigation, as shown in Figure 8.

XRD Study

Figure 9 shows peaks at position 5 (2Theta) with intensity of 3000, 14(2Theta) with intensity of 2500, 16(2Theta) with intensity of 4800, 19(2Theta) with intensity of 1800, 20(2Theta) with intensity of 2000, 27(2Theta) with intensity of 1600, 31(2Theta) with intensity of 900, 33(2Theta) with intensity of 1000. Figure 10 shows the XRD study, highlighted significant characteristic drug peaks at positions 21.06 and 23.63 (2Theta). Such shifts as seen in pure TC were indicated by those peaks. However, a broad peak at 2800 was detected, which might be due to the presence of solvent as well as the finite distribution of the drug in the dosage development.

Surface Morphology of Optimized Formulation

SEM study discovered the presence of optimized lipid nanoparticles, which are sphere-shaped and their surface feature is a smooth surface, as shown in Figure 11.

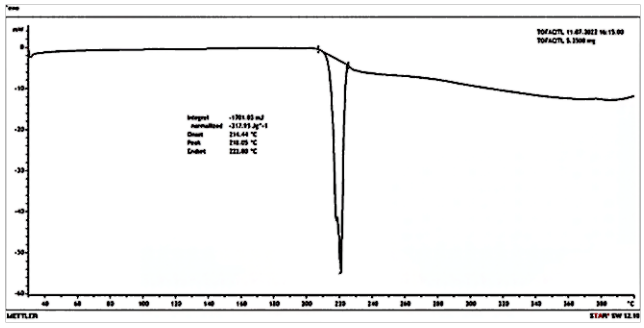

Figure 7: DSC of tofacitinib citrate

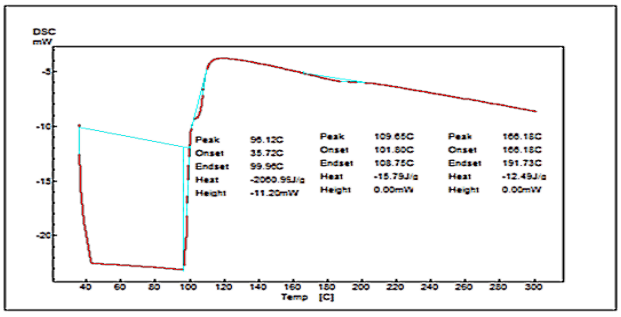

Figure 8: DSC of optimized formulation

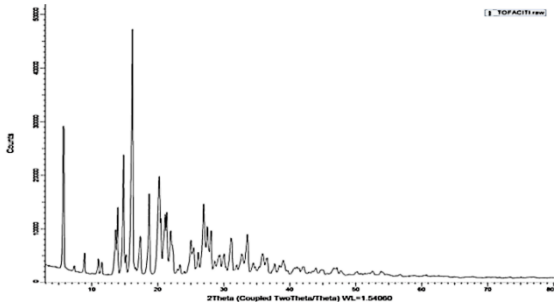

Figure 9: XRD of tofacitinib citrate

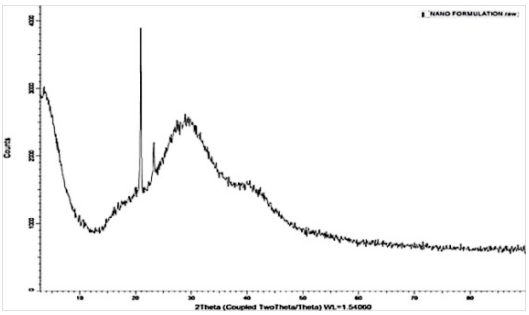

Figure 10: XRD spectra of optimized nanoparticle

Particle Size and Zeta Potential of Optimized Formulation

The optimized formulation's average size was 181.5 nm shown in Figure 12. According to this, a value of 0.495 was found for

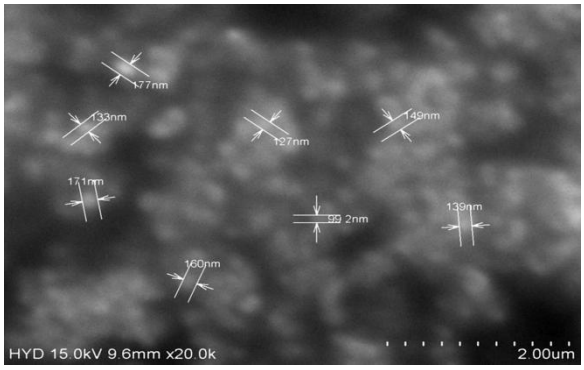

Figure 11: SEM study of optimized formulation

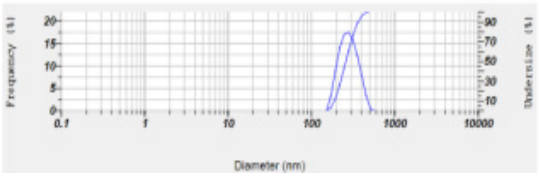

Figure 12: Particle size and distribution study of optimized formulation

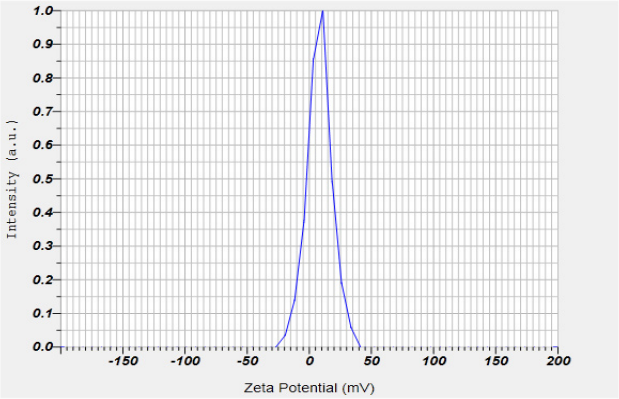

Figure 13: Zeta potential of optimized formulation

the polydispersity index (PI). According to the literature.[63,64] homogeneous dispersion is indicated by a PI value of less than 0.5. Homogeneous dispersion was acquired from the data.

Figure 13 showed a zeta value of 8.2 mV, indicating stability. The zeta potential can further be improved by adding oppositely charged electrolytes. The literature review already stated that the values above ± 15mV are stable and can be dispersed without raising the stability issue.

CONCLUSION

It was found that the Microemulsification technique was effective in successfully incorporating TC with a high entrapment efficiency. Additionally, it stands to reason that the bioavailability might be increased if particles in the nanometer range were obtained. Thus, we may conclude that solid lipid nanoparticles offer controlled drug release. These systems are employed as drug carriers for lipophilic pharmaceuticals and as a means of improving the bioavailability of drugs using nanoparticles as a drug delivery mechanism.

REFERENCES

1. Taylor P.C., Moore A., Vasilescu R., Alvir J., Tarallo M. A structured literature review of the burden of illness and unmet needs in patients with rheumatoid arthritis: a current perspective. Rheumatol. Int. 2016;36(5):685–695.
2. Swapna. S, Dr. R. Shyam Sunder. A Novel Nasal Fluoxetine loaded Solid Lipid Nanoparticles in Mucoadhesive in situ gel Formulation for brain targeting: Preparation, Characterization and in vivo evaluation. YMER. 2022; 21(9):433-452.
3. Dorner T., Strand V., Cornes P., Goncalves J., Gulacsi L., Kay J., Kvien T.K., Smolen J., Tanaka Y., Burmester G.R. The changing landscape of biosimilars in rheumatology. Ann. Rheum Dis. 2016;75(6):974–982.
4. Weber, S., Zimmer, A., & Pardeike, J. Solid Lipid Nanoparticles (SLN) and Nanostructured Lipid Carriers (NLC) for pulmonary application: A review of the state of the art. European Journal of Pharmaceutics and Biopharmaceutics. 2014; 86(1), 7–22
5. Babu VN, Rao GSNK, Budha RR, Alavala RR, Desu PK, Babu GK, Prasad AD. Development, characterization and optimization of solid lipid nanoparticles of alpha-mangostin by central composite design approach. J Appl Pharm Sci, 2023; 13(08):140–150.
6. Swagata Patra, Joykrishna Dey, Avik Chakraborty. Physicochemical Characterization, Stability, and *In-vitro* Evaluation of Curcumin-Loaded Solid Lipid Nanoparticles Prepared Using Biocompatible Synthetic Lipids. ACS Applied Bio Materials. **2023;** *6* (7): 2785-2794.
7. Michael Jackson Ferreira da Silva, Alisson Mendes Rodrigues, Maria Célia Pires Costa, Adriana Leandro Camara. Solid Lipid Nanoparticles Based on Babassu Oil and Copaiba Oleoresin: A Promising Approach for Prostate Cancer Therapy. Nanomaterials **2024**, *14* (12) , 1014.
8. Bhamidipati PK, Kantarjian H, Cortes J, Cornelison AM, Jabbour E. Management of imatinib-resistant patients with chronic myeloid leukemia. Ther Adv Hematol. 2013;4(2):103-17.
9. Xia B, Heimbach T, He H, Lin TH. Nilotinib preclinical pharmacokinetics and practical application toward clinical projections of oral absorption and systemic availability. Biopharm Drug Dispos. 2012;33(9):536-49.
10. Tanaka MF, Kantarjian H, Cortes J, Ohanian M, Jabbour E. Treatment options for chronic myeloid leukemia. Expert Opin Pharmacother. 2012 Apr 1;13(6):815-28.
11. Markovic M, Ben-Shabat S, Aponick A, Zimmermann EM, Dahan A. Lipids and lipid-processing pathways in drug delivery and therapeutics. Int J Mol Sci. 2020 Jan;21(9):3248.
12. Kakodkar S, Sharmada S. Pharmaceutical quality-by-design (QbD): basic principles. Int J Res Methodol. 2015;1(1).
13. Grana A, Limpach A, Chauhan H. Formulation considerations and applications of solid lipid nanoparticles. Am Pharm Rev. 2013;16(1):19-25.
14. Pooja D, Kulhari H, Tunki L, Chinde S, Kuncha M, Grover P, Rachamalla SS, Sistla R. Nanodrugs for targeted delivery of etoposide to non-small cell lung cancer using transferrin-functionalized nanoparticles. RSC Adv. 2015;5(61):49122-31.
15. Barman RK, Iwao Y, Funakoshi Y, Ranneh AH, Noguchi S, Wahed MI, Itai S. Development of highly stable nifedipine solid lipid nanoparticles. Chem Pharm Bull (Tokyo). 2014;62(5):399-406.
16. Shen J, Burgess DJ. *In-vitro* dissolution testing strategies for

nanoparticulate drug delivery systems: recent developments and challenges. Drug Deliv Transl Res. 2013;3(5):409-15.
17. Begum MY, Gudipati PR. Formulation and evaluation of dasatinib-loaded solid lipid nanoparticles. Int J Pharm Pharm Sci. 2018;10(12):14.
18. Taraka Sunil Kumar K, Mohan Varma M, Ravi Prakash. Development and optimization of enzalutamide-loaded solid lipid nanoparticles using box–behnken design. Asian J Pharm Clin Res. 2019;12:67-76.
19. Sawant P, Karekar P, Waghmare K. Formulation and characterization of solid lipid nanoparticles containing ginger oil for enhancement of stability. Int J Pharm Pharm Sci. 2020;12(6):36-44.
20. Fearon U., Canavan M., Biniecka M., Veale D.J. Hypoxia, mitochondrial dysfunction and synovial invasiveness in rheumatoid arthritis. Nat. Rev. Rheumatol. 2016;12:385–397.
21. R. Shyam Sunder, Vasudha Bakshi. Design, *in-vitro* characterization & optimization of mefenamic acid-loaded carboxy methyl chitosan nanoparticles. Journal of Global Trends in Pharmaceutical Sciences. 2020; 11(1):7290-7297.
22. Svendsen A.J., Junker P., Houen G., Kyvik K.O., Nielsen C., Skytthe A., Holst R. Incidence of chronic persistent rheumatoid arthritis and the impact of smoking: a historical twin cohort study. Arthritis Care Res. 2016;69(5):616–624.
23. Yang M., Feng X., Ding J., Chang F., Chen X. Nanotherapeutics relieve rheumatoid arthritis. J. Control Release. 2017;252:108–124.
24. McInnes I.B., Schett G. Pathogenetic insights from the treatment of rheumatoid arthritis. Lancet. 2017;389:2328–2337.
25. Ursini F., Leporini C., Bene F., D'Angelo S., Mauro D., Russo E., De Sarro G., Olivieri I., Pitzalis C., Lewis M., Grembiale R.D. Anti-TNF-alpha agents and endothelial function in rheumatoid arthritis: a systematic review and meta-analysis. Sci. Rep. 2017;7:5346.
26. Tanaka Y. Current concepts in the management of rheumatoid arthritis. Korean J. Intern. Med. 2016;31(2):210–218.
27. McInnes I.B., Schett G. Pathogenetic insights from the treatment of rheumatoid arthritis. Lancet 2017;389:2328–2337.
28. Jones G., Nash P., Hall S. Advances in rheumatoid arthritis. Med. J Aust. 2017;206(5):221–224.
29. Dodle Trishala, Bichitrananda Tripathy, Swapna S. A Critical Review on Phytosomes: Advancement and Research on Emerging Nanotechnological Tools. Current Bioactive Compounds.2023;19(5):89-99.
30. J. Rajkumar, Dr.Akiful Haque, Swapna.S. Characterization and Optimization of Hydrogel Films Loaded with a Hydrophobic Drug. Eur. Chem. Bull.2023; 12(9):3347-3363.
31. Bhalekar M.R., Madgulkar A.R., Desale P.S., Marium G. Formulation of piperine solid lipid nanoparticles (SLN) for treatment of rheumatoid arthritis. Drug. Dev. Ind Pharm. 2017;43(6):1003–1010.
32. Raj R., Mongia P., Ram A., Jain N.K. Enhanced skin delivery of aceclofenac via hydrogel-based solid lipid nanoparticles. Artif. Cells Nanomed. Biotechnol. 2016;44(6):1434–1439.
33. Garg N.K., Singh B., Tyagi R.K., Sharma G., Katare O.P. Effective transdermal delivery of methotrexate through nanostructured lipid carriers in an experimentally induced arthritis model. Colloids Surf. B Biointerfaces. 2016;147:17–24.
34. Chavan D., Gangode B., Jadhav A., Patil M., Kshirsagar S. Solid lipid nanoparticles: a modern formulation approach in drug delivery system. IJOD. 2017;5(2):56–70.
35. Panahi Y., Farshbaf M., Mohammadhosseini M., Mirahadi M., Khalilov R., Saghfi S., Akbarzadeh A. Recent advances on liposomal nanoparticles: synthesis, characterization and biomedical applications. Artif. Cells Nanomed. Biotechnol. 2017;45(4):788–799.
36. R. Saitejaswi, Swapna. S. Formulation and Evaluation of Lornoxicam loaded Transfersome gel. European Journal of Biomedical and Pharmaceutical Sciences. 2016; 3(3):144-150
37. Heloise R., Danhier F., Preat V., Langer R., Anderson D.G. Nanoparticle-based drug delivery systems: a commercial and regulatory outlook as the field matures. Expert Opion Drug Deliv. 2017;14(7):851–864.
38. P. Nagendrababu, Vasudha Bakshi. Augmentation of Solubility of Carvedilol Phosphate by Solid Dispersions Using Skimmed Milk. Indo-American Journalof Pharmaceutical Research. 2015; 5: 3521-27
39. Dolati S., Sadreddini S., Rostamzadeh D., Ahmadi M., Jadidi-Niaragh F., Yousefi M. Utilization of nanoparticle technology in rheumatoid arthritis treatment. Biomed. Pharmacother. 2016;80:30–41.
40. Nogueira E., Gomes A.C., Preto A., Cavaco-Paulo A. Folate-targeted nanoparticles for rheumatoid arthritis therapy. Nanodrug. 2016;12(4):1113–1126.
41. Bianchi G., Caporali R., Todoerti M., Mattana P. Methotrexate and rheumatoid arthritis: current evidence regarding subcutaneous versus oral routes of administration. Adv. Ther. 2016;33(3):369–378.
42. Li H.Z., Xu X.H., Lin N., Lu H.D. Metabolic and cardiovascular benefits of hydroxychloroquine in patients with rheumatoid arthritis: a systematic review and meta-analysis. Ann. Rheum Dis. 2018;77(1):98–103.
43. Bahadar H., Maqbool F., Niaz K., Abdollahi M. Toxicity of nanoparticles and an overview of current experimental models. Iran Biomed. J. 2016;20(1):1–11.
44. Ramaiah Maddi, Balaji Maddiboyina, Ramya Krishna Nakkala, Harekrishna Roy, M Akiful Haque, Azmath Farhana, & Swapna S. Exploring the Therapeutic Potential of Probiotics in Fighting Respiratory Viral Infections. Journal of Population Therapeutics and Clinical Pharmacology, 2022; 29(04), 886–900.